HOSTED BY

ELSEVIER

Available at www.sciencedirect.com

ScienceDirect

journal homepage: www.elsevier.com/locate/IJMYCO

Computational approach to understanding the mechanism of action of isoniazid, an anti-TB drug

Lingaraja Jena [a], *Pranita Waghmare* [a], *Supriya Kashikar* [b], *Satish Kumar* [a], *Bhaskar C. Harinath* [a,*]

[a] *Bioinformatics Centre, Biochemistry & JBTDRC, MGIMS, Sevagram, Maharashtra, India*
[b] *GeNext Genomics Pvt. Ltd., Nagpur, Maharashtra, India*

ARTICLE INFO

Article history:
Received 2 August 2014
Accepted 5 August 2014
Available online 2 September 2014

Keywords:
Isoniazid
KatG
InhA
Drug resistance
Mutation

ABSTRACT

Tuberculosis (TB) is an ancient disease caused by *Mycobacterium tuberculosis* (MTB), which remains a major cause for morbidity and mortality in several developing countries. Most drug-resistant MTB clinical strains are resistant to isoniazid (INH), a first-line anti-TB drug. Mutation in KatG, a catalase-peroxidase, of MTB is reported to be a major cause of INH resistance. Normally upon activation by KatG, INH is converted to an active intermediate which has antimycobacterial action in MTB. This INH intermediate in the presence of NADH forms INH-NAD adduct which inhibits inhA (2-trans-enoyl-acyl carrier protein reductase) of MTB, thus blocking the synthesis of mycolic acid, a major lipid of the mycobacterial cell wall. In this docking study, the high binding affinity of INH-NAD adduct towards InhA was observed in comparison with INH alone. In this study, two resistant mutants of KatG (S315T and S315N) were modeled using Modeller9v10 and docking analysis with INH was performed using AutoDock4.2 and the docking results of these mutants were compared with the wild type KatG. Docking results revealed the formation of a single hydrogen (H) bond between the secondary amine nitrogen (–NH) of INH with Thr or Asn residues in place of Serine at 315 position of KatG mutant strains respectively, whereas in the case of the wild type, there was no H-bond formation observed between INH and Ser315. The H-bond formation may prevent free radical formation by KatG in mutant strains thus the development of resistance to the drug. This *in silico* evidence may implicate the basis of INH resistance in KatG mutant strains.

Introduction

Decades after the discovery of the *Mycobacterium tuberculosis* (MTB) organism, tuberculosis (TB) remains a major cause of morbidity and mortality in several developing countries. Nearly 33% of the world's population is considered to be infected with MTB infection, with 8.6 million new patients and 1.3 million deaths in the year 2012, including 320,000

* Corresponding author. Address: JB Tropical Disease Research Centre, Mahatma Gandhi Institute of Medical Sciences, Sevagram 442 102, Wardha, Maharashtra, India. Tel.: +91 7152 284341/284355x262, 303; fax: +91 (07152) 284038.
E-mail addresses: bc_harinath@yahoo.com, info@jbtdrc.org (B.C. Harinath).
http://dx.doi.org/10.1016/j.ijmyco.2014.08.003

deaths among HIV-positive individuals. In India alone, there were 2.0 million to 2.4 million infected cases of TB, i.e., 26% of total cases [1]. Multi-drug-resistant strains of this pathogen, emerging in association with HIV, have added a frightening dimension to the problem [2]. Outbreaks of extensively drug-resistant (XDR) tuberculosis have also been an increasing threat in certain regions around the world [3]. Most drug-resistant MTB clinical strains are resistant to isoniazid (INH, isonicotinic acid hydrazine) – a first-line, anti-tuberculous drug [4].

Isoniazid (INH), also known as isonicotinyl hydrazine, is an organic compound used as a first-line drug in the prevention and treatment of TB. It has a simple structure (Fig. 1) containing two essential components required for the high activity against MTB, i.e., a pyridine ring and a hydrazide group [5]. This compound was first synthesized in the early 20th

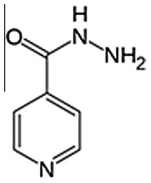

Fig. 1 – Chemical structure of Isoniazid (Formula: $C_6H_7N_3O$; Mol. Wt.: 137.139 g/mol).

Table 1 – Proteins of *Mycobacterium tuberculosis* reported to associate with Isoniazid resistance.

Locus_tag	Name	Protein length	Locus	PDB ID	Mutation
Rv1772	Hypothetical protein Rv1772	103	–	–	Thr4Ala
Rv1909c	Ferric uptake regulation protein furA (fur)	150	furA	–	Ser5Pro
Rv0340	Hypothetical protein Rv0340	179	–	–	Val163Ile
Rv2428	Alkyl hydroperoxide reductase subunit C	195	ahpC	2BMX	Inter-genic region G(−46)A
Rv1483	3-Oxoacyl-[acyl-carrier-protein] reductase	247	fabG1	1UZL	Ala5Pro, Val14Leu, Thr21Ala
Rv1484	Enoyl-(acyl carrier protein) reductase	269	inhA	1P44	Lys8Asn, Ile16Thr, Ile21Val/Thr, Ile47Thr, Val78Ala, Ser94Ala/Leu, Ile95Pro, Ile95Thr, Ile194Thr, Arg202Gly, Glu217Asp, promoter region
Rv3566c	Arylamine n-acetyltransferase nat	283	nat	4BGF	Gly67Arg, Gly207Glu
Rv2243	Acyl-carrier-protein S-malonyltransferase	302	fabD	2QC3	Ser275Asn
Rv0129c	Secreted antigen 85-C FBPC (85C) (antigen 85 complex C) (AG58C) (fibronectin-binding protein C)	340	fbpC	4MQM	Gly158Ser −63(C/T), −23(A/C)
Rv2242	Hypothetical protein Rv2242	414	–	–	Asp3Gly, Met323Thr
Rv2245	3-Oxoacyl-(acyl carrier protein) synthase II	416	kasA	4C6U	Asp66Asn, Met77Ile, Arg121Lys, Gly269Ser,Gly312Ser, Gly387Asp, Phe413Leu
Rv1592c	Hypothetical protein Rv1592c	446	–	–	Pro42Leu, Val430Ala
Rv1854c	NADH dehydrogenase	463	ndh	–	Arg13Cys, Val18Ala, Thr110Ala, Leu239Pro, Arg268His
Rv3139	Acyl-CoA dehydrogenase FADE24	468	fadE24	–	Insertion of 2 base pair (bp) at nucleotide position -64
Rv2247	Acetyl/propionyl-CoA carboxylase beta subunit AccD6	473	accD6	4FB8	Asp229Gly
Rv0341	Isoniazid inducible gene protein INIB	479	iniB	–	Deletion of 12 bp at nucleotide position 665
Rv0343	Isoniazid inducible gene protein INIC	493	iniC	–	Trp83Gly
Rv2846c	Integral membrane efflux protein EfpA	530	efpA	–	Ile73Thr
Rv0342	Isoniazid inducible gene protein INIA	640	iniA	–	Pro3Ala, Arg537His
Rv1908c	Catalase–peroxidase-peroxynitritase T KatG	740	katG	2CCA	Ser315Thr, Ser315Asn, Arg463Leu, Ser17Asn, Gly19Asp, Ser140Asn/Arg, Gly279Asp, Gly285Asp, Gly316Asp, Ser457Ile, Gly593Asp
Rv3795	Integral membrane indolylacetylinositol arabinosyltransferase EMBB	1098	embB	–	Tyr333His
Rv2427a	Transcriptional regulator OxyR′, pseudogene		oxyR′	–	–

century, and its activity against TB was first reported in the early 1950s [6]. With the introduction of isoniazid, TB treatment was first considered feasible. Isoniazid inhibits the synthesis of mycolic acids, an essential component of the bacterial cell wall. At therapeutic levels isoniazid is bactericidal against actively growing intracellular and extracellular MTB organisms. Isoniazid is used in conjunction with other effective anti-tuberculosis agents under multi-drug therapy [7].

Isoniazid is one of the most effective anti-TB drugs used for TB treatment. This pro-drug requires activation, which is carried out by the heme enzyme catalase/peroxidase (KatG) of MTB. The mechanism of activation has not yet been clearly understood as the binding interaction has not been appropriately established [8]. Besides, InhA (2-trans-enoyl-acyl carrier protein reductase) of MTB is a well-known target of INH [4]; a few other targets have also been proposed in order to explain the atypical potency of isoniazid [9].

Mechanisms of action of isoniazid

The mechanism of INH action has been the subject of rigorous studies, but it is reported to generate a variety of highly reactive compounds, including reactive oxygen species (ROS) such as superoxide, peroxide and hydroxyl radical [10], and nitric oxide [11]; reactive organic species such as isonicotinic acyl radical or anion [12]; and certain electrophilic species [13], which then attack multiple targets in MTB [14].

INH passively diffuses through the mycobacterial envelope, is activated by $MnCl_2$ and the catalase–peroxidase KatG, possibly into an isonicotinoyl radical or anion, which then inhibits the InhA through a covalent attachment to NADH within the active site of the protein. InhA has been shown to preferentially catalyze the NADH-dependent reduction of 2-trans-enoyl-ACP molecules with 16 or more carbons. This reaction corresponds to the final step of elongation of the fatty acid. In addition, INH inhibits the biosynthesis of mycolic acids, which are extremely long chain fatty acids, specific to mycobacteria. A link between the inhibition of InhA and the inhibition of mycolic acid synthesis is provided by the fact that a mutation in the inhA gene, which confers INH resistance, also leads to the inhibition of mycolic acid biosynthesis to INH [4].

Study of the interaction of isoniazid with MTB enzymes through a bioinformatics approach

INH resistance in TB is a complex process. Mutations in several genes, including katG, inhA, ahpC, ndh and kasA, were reported to associate with isoniazid resistance [15]. The rapid

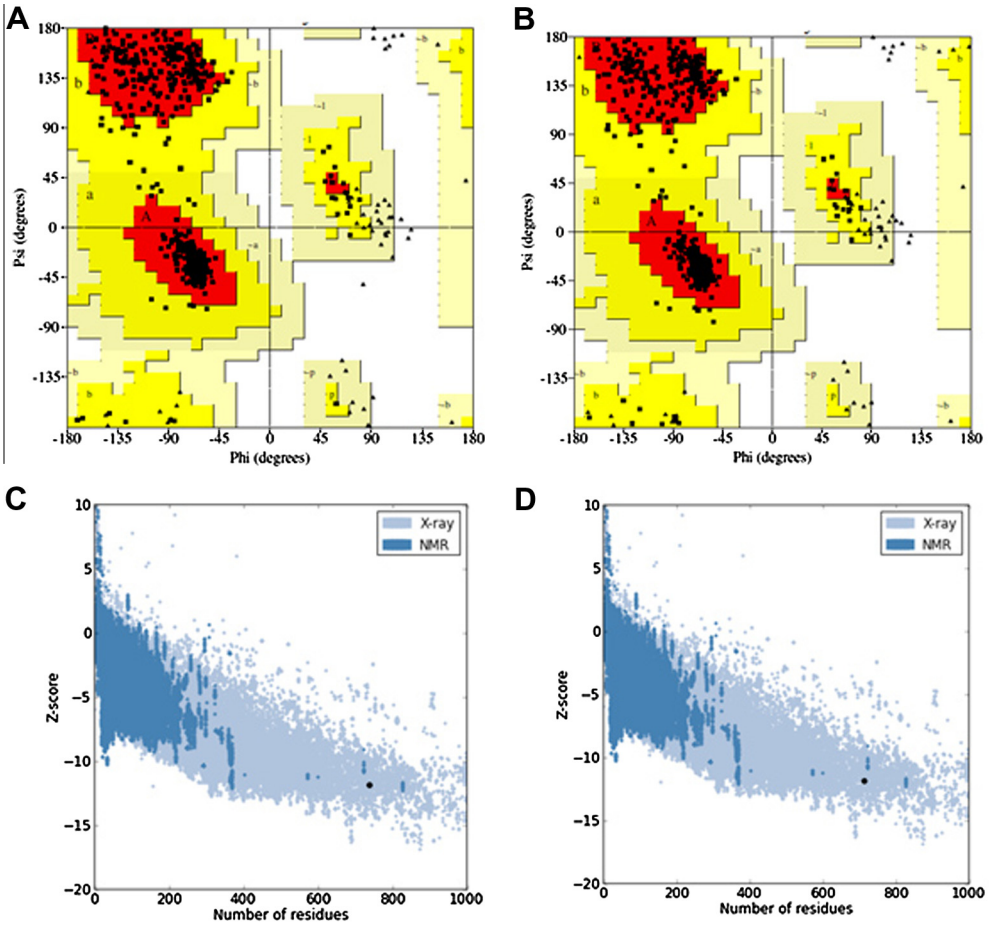

Fig. 2 – (A) Ramachandran plot of predicted KatG (S315T) mutant model. (B) Ramachandran plot of predicted KatG (S315N) mutant model. (C) Z plot of KatG (S315T). (D) Z plot of KatG (S315N) model. ProSA-web Z-scores of all protein chains in PDB, determined by X-ray crystallography and NMR spectroscopy, with respect to their length. The Z-score of KatG mutants were present in that range represented in the black dots.

advances in molecular biology and the accessibility of new information generated after the whole genome sequencing of MTB will be useful in understanding the mechanism of INH resistance.

Sandgren et al. compiled a comprehensive list of the genetic polymorphisms associated with first- and second-line drug resistance in clinical MTB isolates throughout the world and reported that there were 22 genes of MTB which were associated with INH resistance [16]. As per TB drug resistance mutation database [16], 22 genes/proteins of MTB were reported to associate with INH resistance (Table 1). Mutation of amino acids in different enzymes is shown in Table 1. Out of 22 proteins, 9 proteins have a known experimentally determined 3D-structure available at the Protein Data Bank. Two proteins-katG and InhA-are reported to interact with INH. In this study, the interaction of INH with KatG and InhA through molecular docking analysis was explored.

Materials and methods

Hardware and software

The study was carried out on a Dell Workstation with a 2.26 GHz processor, 6 GB RAM and 500 GB hard drive running in a Windows operating system. Bioinformatics software, such as AutoDock4.2 and online resources were used in this study.

M. tuberculosis KatG and InhA protein

Two important proteins of MTB–KatG and InhA-are reported to be directly involved in INH resistance, and the experimentally determined structures of both the proteins obtained through the X-ray diffraction experiment are available at the Protein Data Bank (PDB) [17]. The three-dimensional structure of KatG (PDB ID: 2CCA) and InhA (PDB ID: 1P44) were retrieved from the PDB for docking study. Two mutants of KatG (S315T and S315N) were generated using Modeller9v10 [18].

Ligand preparation

The ligand (INH) used in this study against KatG was retrieved from the PubChem database [19]. INH-NAD adduct was used as another ligand against InhA, and PRODRG2 Server [20] was used to obtain the chemical structure of INH-NAD adduct in PDB format.

Protein–ligand docking

Protein–ligand docking studies were performed using the AutoDock4.2 program [21]. It is one of the most widely used methods for protein–ligand docking. All the pre-processing steps for ligand and protein files were performed using the AutoDock Tools 1.5.4 program (ADT) which has been released as an extension suite to the Python Molecular Viewer [21]. The ADT program was used to prepare receptor molecules (KatG and InhA) by adding all hydrogen atoms into the carbon atoms of the receptor and Kollman charges were also assigned. For docked ligands, non-polar hydrogens were also added. Gasteiger charges were assigned and torsion degrees of freedom were allocated by the ADT program.

The Lamarckian genetic algorithm (LGA) was applied to model the interaction pattern between receptors and the ligand. The grid maps representing the receptor proteins in

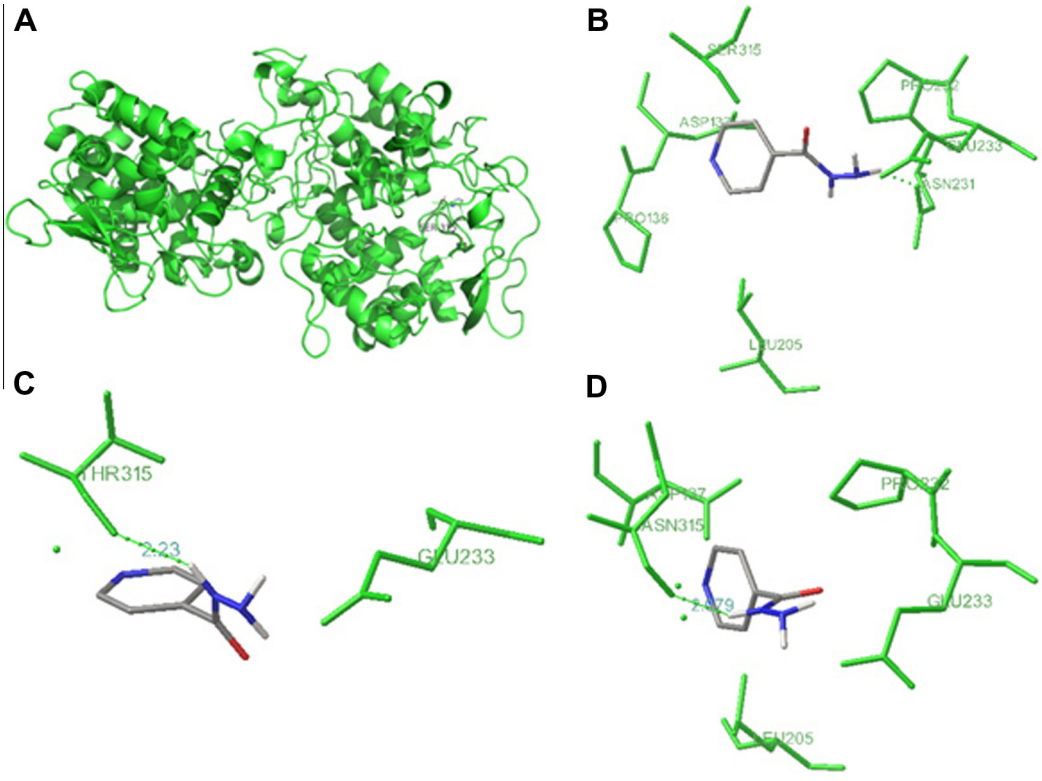

Fig. 3 – (A) 3D structure of KatG; Docking interaction of INH with (B) wild type KatG (no H-bond with Serine315) whereas (C) KatG S315T mutant; and (D) KatG S315N mutant showing hydrogen bonds in dotted lines.

the docking process were calculated using AutoGrid (part of the AutoDock package). A grid of 40, 40 and 40 points in x, y, and z directions was centered on the known active site residues of each protein. For all docking procedures, 10 independent genetic algorithm (GA) runs with population size 150 were considered for each molecule under study. A maximum number of 25×10^5 energy evaluations; 27,000 maximum generations; a gene mutation rate of 0.02 and a crossover rate of 0.8 were used for Lamarckian genetic algorithm. The AutoDock program was run in order to prepare corresponding DLGs (docking log files) for further analysis.

Visualization

The visualization of structure files was done using graphical interface of ADT tool and PyMol molecular graphics system (www.pymol.org).

Results and discussion

Validation of model

KatG of MTB encoded by Rv1908c has 740 amino acids in its protein sequence whereas there are 269 amino acids in the protein sequence of InhA (enoyl-[acyl carrier protein] reductase) encoded by Rv1484. Three-dimensional structures of both the proteins are available at PDB. The single amino acid mutation at codon 315, i.e., Ser to Thr (AGC–ACC) of the KatG gene is reported to be the most widespread mutation, associated with INH resistance [22]. Another mutation, Ser315Asn (AGC/AAC), was also reported in the INH resistance strain [23]. Thus, mutant models of KatG (S315T and S315N) were generated and subjected for validation. The stereochemistry of the KatG (S315T) model (Procheck analysis) revealed that 92.8% of residues were situated in the most favorable region and 7.2% were in additional allowed regions, whereas none of the residues fell in the generously allowed and disallowed region of the Ramachandran plot (Fig. 2A). In the case of the KatG (S315N) model, 93.3% of residues were found in the most favorable region and 6.7% in the additional allowed regions (Fig. 2B). ProSA-web evaluation revealed a compatible Z score value of −11.85 and −11.87 for the KatG (S315T) (Fig. 2C) and the KatG (S315N) (Fig. 2D) models, respectively, which are well within the range of the native conformations of crystal structures [24]. The overall residue energies of both the mutant models were largely negative. The 3D model of both mutants showed an LG score of around 4.8 by the Protein Quality Predictor (ProQ) tool, implying the high accuracy level of the predicted structure. A ProQ LG score >2.5 is necessary for suggesting that a model is of very good quality [25].

Docking analysis of KatG and isoniazid

On the basis of the crystal structure of KatG (PDB ID: 2CCA) (Fig. 3A), three-dimensional structures of two mutants were obtained. The protein (KatGs) – ligand (INH) was performed using AutoDock4.2 software [21]. Out of the ten poses obtained, the best ligand pose was selected based on the lowest binding energy confirmation. As the amino acid (Serine) at 315 position of KatG was reported to have undergone a mutation in most of the INH resistance strains, docking of INH was performed around this amino acid position. Upon docking, INH interacts with the wild type KatG protein with binding energy of −5.36 kcal/mol, whereas in case of KatG (S315T) and KatG (S315N) mutants, the binding energies were found to be −4.98 and −5.15 kcal/mol respectively. However, there was not much variation in the binding energy of the protein–ligand complex in all three cases, but there was no hydrogen bond formation observed between INH with Ser315 residues of wild type KatG (Fig. 3B), while in the case of the mutant strains – KatG (S315T) and KatG (S315N) – there was a hydrogen-bond formation between INH with Thr315 (Fig. 3C) and Asn315 (Fig. 3D) with a bond length of 2.23 and 2.079 Å, respectively.

Timmins et al. [11] demonstrated the generation of nitric oxide upon the activation of INH by KatG (Fig. 4A) [11]. The INH-derived NO· had biological activity and was shown to be involved in antimycobacterial action [11]. In this docking study, it was also revealed that the Threonine residues of the KatG (S315T) mutant (Fig. 4B) and the Asparagine residue of the KatG (S315N) mutant formed one H-bond with -NH atom of INH. As the hydrogen bond formation has shown to

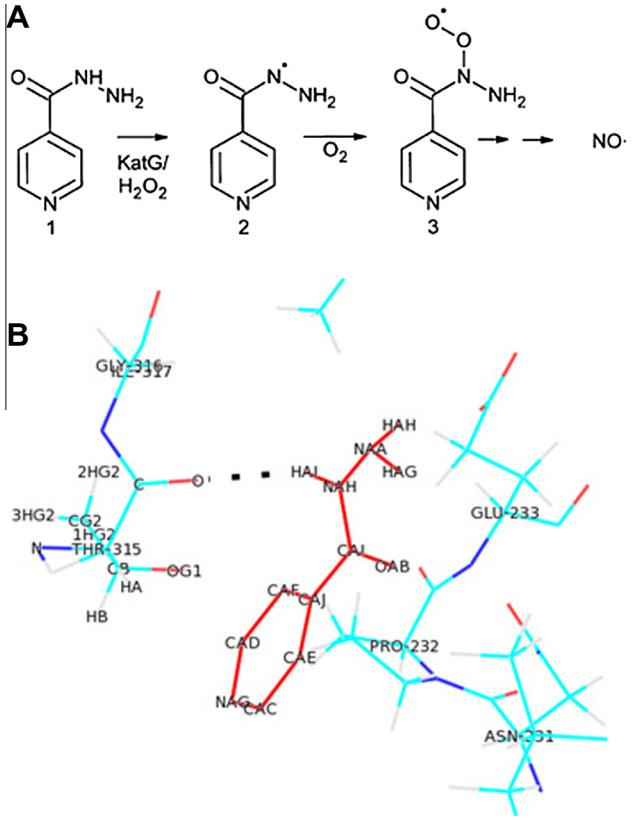

Fig. 4 – (A) Radical formation in the presence of Serine (wild type strain) (Postulated pathway of NO· production. Oxidation of INH (1) at N2 to form the hydrazyl radical (2) is followed by oxygen addition to the hydrazyl radical (causing N–O bond formation) (3), followed by as yet undelineated fragmentation or elimination [11]; (B) H-bond formation (between –CO of Thr315 and –NH of INH) and prevention of a radical formation in the presence of Threonine in place of Serine (resistant strain).

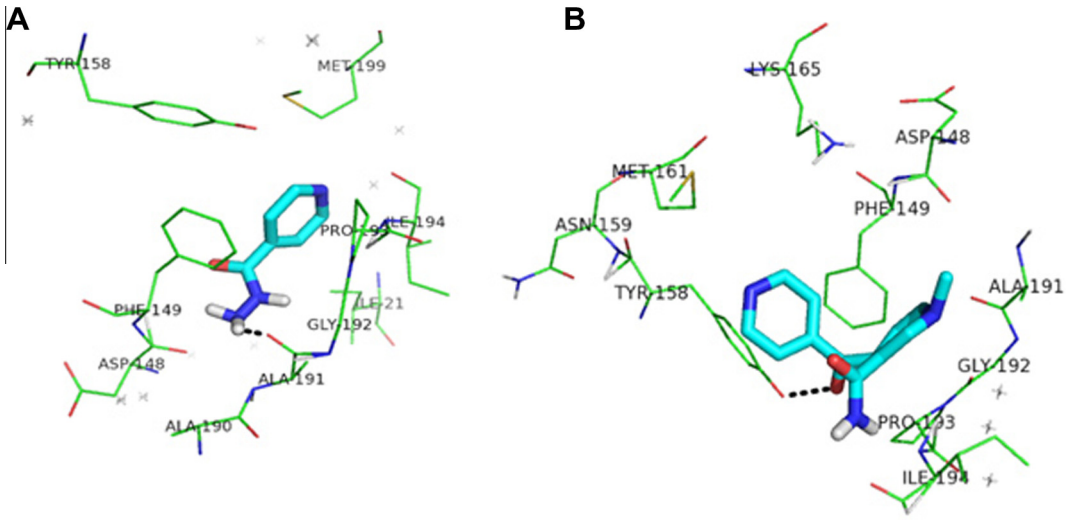

Fig. 5 – Docking of InhA with (A) isoniazid (INH) (with binding energy of −4.75 kcal/mol) and (B) INH-NAD (with binding energy of −6.25 kcal/mol).

have radical scavenging activity [26], this may prevent free radical formation in the mutant strains that may lead to INH resistance.

Docking analysis of InhA and INH/INH-NAD adduct

INH was reported to act on *M. tuberculosis* by inhibiting a 2-trans-enoyl-acyl carrier protein reductase, called InhA encoded by Rv1484 [4]. INH-NAD adduct was also reported as a capable InhA inhibitor [27,28]. In this study, docking analysis was performed between InhA with INH and INH-NAD adduct separately. Tyr158 of InhA is reported as an important binding site residue that interacts with the long chain fatty acyl substrates, required for the synthesis of mycolic acids, a major component of mycobacterial cell walls [29]. Docking of InhA with isoniazid/INH-NAD adduct was performed around substrate binding residue Tyr158. Isoniazid binds with InhA with binding energy of −4.75 kcal/mol and the inhibition constant of the protein–ligand complex (Fig. 5A) was found to be 328.38 μM, while INH-NAD adduct binds with InhA with the lowest binding energy of −6.25 kcal/mol as compared with INH only. INH-NAD adduct also formed one H-bond with a known binding site residue Tyr158 (Fig. 5B). This docking analysis revealed that the INH-NAD adduct had more binding affinity towards InhA with the inhibition constant of 26.4 μM, as compared with INH. This *in silico* docking study correlates with an earlier *in vitro* study by Nguyen et al. reporting that the INH-NAD adduct as a powerful inhibitor of InhA [27].

Conclusion

The computational approach has been employed to study the interaction between INH with KatG and its mutant models. The *in silico* docking study revealed that the mutation in KatG at amino acid position 315 (S315T/S315N) might be involved in hydrogen bond formation between INH with mutant Thr(T)/Asn(N) residues. This H-bond formation may hamper INH-derived free radical formation. In wild type KatG, no H-bond formation occurred between Ser315 residue and INH that may lead to free radical formation which may be toxic to mycobacterium. Furthermore, the interaction between INH and INH-NAD adduct with InhA showed that the INH-NAD adduct is more effectively inhibiting InhA. This toxic consequence of INH with other MTB proteins needs to be explored further in order to design novel drugs against the pathogen.

Conflict of interest

None declared.

Acknowledgements

The authors thank the Department of Biotechnology, Ministry of Science & Technology, Government of India for financial support to Bioinformatics Centre wherein this study has been carried out. The authors convey thanks to Shri Dhiru S. Mehta, President, KHS for his keen interest and encouragement.

REFERENCES

[1] World Health Organization, WHO Global Tuberculosis Report 2013 (2013).
[2] M.C. Raviglione, D.E. Snider Jr., A. Kochi, Global epidemiology of tuberculosis. Morbidity and mortality of a worldwide epidemic, JAMA 273 (1995) 220–266.
[3] N.S. Shah, A. Wright, G.H. Bai, L. Barrera, F. Boulahbal, N. Martín-Casabona, et al, Worldwide emergence of extensively drug-resistant tuberculosis, Emerg. Infect. Dis. 13 (2007) 380–387.
[4] H. Marrakchi, G. Lanéelle, A. Quémard, InhA, a target of the antituberculous drug isoniazid, is involved in a mycobacterial

fatty acid elongation system, FAS-II, Microbiology 146 (2000) 289–296.
[5] G. Middlebrook, M.L. Cohn, Some observations on the pathogenicity of isoniazid-resistant variants of tubercle bacilli, Science 118 (1953) 297–299.
[6] H.L. Rieder, Fourth-generation fluoroquinolones in tuberculosis, Lancet 373 (2009) 1148–1149.
[7] <http://www.rxlist.com/isoniazid-drug/clinical-pharmacology.htm>, 2014 (accessed 15.07.14).
[8] C. Metcalfe, I.K. Macdonald, E.J. Murphy, K.A. Brown, E.L. Raven, P.C. Moody, The tuberculosis prodrug isoniazid bound to activating peroxidases, J. Biol. Chem. 283 (2008) 6193–6200.
[9] T. Scior, I. Meneses Morales, S.J. Garcés Eisele, D. Domeyer, S. Laufer, Antitubercular isoniazid and drug resistance of *Mycobacterium tuberculosis*—a review, Arch. Pharm. 335 (2002) 511–525.
[10] H.A. Shoeb, B.U. Bowman Jr., A.C. Ottolenghi, A.J. Merola, Peroxidase-mediated oxidation of isoniazid, Antimicrob. Agents Chemother. 27 (1985) 399–403.
[11] G.S. Timmins, S. Master, F. Rusnak, V. Deretic, Nitric oxide generated from isoniazid activation by KatG: source of nitric oxide and activity against *Mycobacterium tuberculosis*, Antimicrob. Agents Chemother. 48 (2004) 3006–3009.
[12] R. Rawat, A. Whitty, P.J. Tonge, The isoniazid-NAD adduct is a slow, tight-binding inhibitor of InhA, the *Mycobacterium tuberculosis* enoyl reductase: adduct affinity and drug resistance, Proc. Natl. Acad. Sci. U.S.A. 100 (2003) 13881–13886.
[13] K. Johnsson, D. King, P. Schultz, Studies on the mechanism of action of isoniazid and ethionamide in the chemotherapy of tuberculosis, J. Am. Chem. Soc. 117 (1995) 5009–5010.
[14] L.C. Santos, Review: the molecular basis of resistance in *Mycobacterium tuberculosis*, OJMM 2 (2012) 24–36.
[15] P.E. Almeida Da Silva, J.C. Palomino, Molecular basis and mechanisms of drug resistance in *Mycobacterium tuberculosis*: classical and new drugs, J. Antimicrob. Chemother. 66 (2011) 1417–1430.
[16] A. Sandgren, M. Strong, P. Muthukrishnan, B.K. Weiner, G.M. Church, M.B. Murray, Tuberculosis drug resistance mutation database, PLoS Med. 6 (2009) e2.
[17] H.M. Berman, T. Battistuz, T.N. Bhat, W.F. Bluhm, P.E. Bourne, K. Burkhardt, et al, The Protein Data Bank, Acta Crystallogr., Sect. D: Biol. Crystallogr. 58 (2002) 899–907.
[18] N. Eswar, D. Eramian, B. Webb, M.Y. Shen, A. Sali, Protein structure modeling with MODELLER, Methods Mol. Biol. 426 (2008) 145–159.
[19] Y. Wang, J. Xiao, T.O. Suzek, J. Zhang, J. Wang, S.H. Bryant, PubChem: a public information system for analyzing bioactivities of small molecules, Nucleic Acids Res. 37 (2009) W623–W633.
[20] A.W. Schüttelkopf, D.M. van Aalten, PRODRG: a tool for high-throughput crystallography of protein-ligand complexes, Acta Crystallogr., Sect. D: Biol. Crystallogr. 60 (2004) 1355–1363.
[21] G.M. Morris, R. Huey, W. Lindstrom, M.F. Sanner, R.K. Belew, D.S. Goodsell, et al, AutoDock4 and AutoDockTools4: automated docking with selective receptor flexibility, J. Comput. Chem. 30 (2009) 2785–2791.
[22] S. Ramaswamy, J.M. Musser, Molecular genetic basis of antimicrobial agent resistance in *Mycobacterium tuberculosis*: 1998 update, Tuber. Lung. Dis. 79 (1998) 3–29.
[23] W.H. Haas, K. Schilke, J. Brand, B. Amthor, K. Weyer, P.B. Fourie, et al, Molecular analysis of katG gene mutations in strains of *Mycobacterium tuberculosis* complex from Africa, Antimicrob. Agents Chemother. 41 (1997) 1601–1603.
[24] M. Wiederstein, M.J. Sippl, ProSA-web: interactive web service for the recognition of errors in three-dimensional structures of proteins, Nucleic Acids Res. 35 (2007) W407–W410.
[25] B. Wallner, A. Elofsson, Can correct protein models be identified?, Protein Sci 12 (2003) 1073–1086.
[26] L. Mathiesen, K.E. Malterud, R.B. Sund, Hydrogen bond formation as basis for radical scavenging activity: a structure-activity study of C-methylated dihydrochalcones from Myrica gale and structurally related acetophenones, Free Radic. Biol. Med. 22 (1997) 307–311.
[27] M. Nguyen, A. Quemard, S. Broussy, J. Bernadou, B. Meunier, Mn(III) pyrophosphate as an efficient tool for studying the mode of action of isoniazid on the InhA protein of *Mycobacterium tuberculosis*, Antimicrob. Agents Chemother. 46 (2002) 2137–2144.
[28] D.A. Rozwarski, G.A. Grant, D.H. Barton, W.R. Jacobs Jr., J.C. Sacchettini, Modification of the NADH of the isoniazid target (InhA) from *Mycobacterium tuberculosis*, Science 279 (1998) 98–102.
[29] D.A. Rozwarski, C. Vilchèze, M. Sugantino, R. Bittman, J.C. Sacchettini, Crystal structure of the *Mycobacterium tuberculosis* enoyl-ACP reductase, InhA, in complex with NAD+ and a C16 fatty acyl substrate, J. Biol. Chem. 274 (1999) 15582–15589.